e-J. Surf. Sci. Nanotech. Vol. 10 (2012) 471-475 Conference - ISSS-6 -

Thermoelectric Properties in Transparent-Conductive Cerium-Doped In_2O_3 Films*

Natsuki Mori,† Junichi Ueno,‡ and Yusuke Uesugi
Department of Electrical and Computer Engineering,
Oyama National College of Technology, 771 Nakakuki, Oyama, Tochigi 323-0806, Japan

Kazushi Miki
National Institute for Materials Science (NIMS),
1-1 Namiki, Tsukuba, Ibaraki 305-0044, Japan, and
Graduate School of Pure and Applied Sciences, University of Tsukuba,
1-1 Tennodai, Tsukuba, Ibaraki 305-8573, Japan

(Received 31 January 2012; Accepted 10 July 2012; Published 1 September 2012)

Thermoelectric properties are studied in Ce-doped In_2O_3 (ICO) films with Ce content x up to 9 at.% prepared by dc sputtering. Films of ICO are transparent in the visible light region (transmission more than 80%), having the highest room-temperature conductivity σ_{300}=120 S/cm for $x = 3$ at.%. Thermoelectric power at room temperature S_{300} is well correlated to the electron density n, showing a linear relation of S_{300} vs. $\ln(\sigma_{300})$ in the Jonker fashion. The temperature dependence of the thermoelectric power $S(T)$ is well described in terms of a simple percolation model characterized by a formula $S_p(T) = AT + (B/T) + C$ with fitting parameters A, B and C. We define a percolation index as $\Gamma_{300} = |B/(AT^2)|$ at $T = 300$ K, the doping dependence of which is found to be related to that of the power factor $P_{300} = S_{300}^2 \cdot \sigma_{300}$ in the ICO films. Similar correlations are also shown in bulk-systems composed of rare-earth metal oxides. [DOI: 10.1380/ejssnt.2012.471]

Keywords: Electrical transport measurements; Indium oxide; Ceramic thin films; Thermoelectric properties; Transparent-conductive films; Percolation

I. INTRODUCTION

It is well known that indium oxide (In_2O_3) has been playing a central role as a host material of transparent-conductive films [1]. Among many kinds of impurity elements, it appears that there is no dopant superior than tin atoms [1, 2]. In recent years, much effort has been devoted to studies of impurity effects in indium oxides with transition metal (TM) elements, such as Mo [3], Ti [4] and Zr [5]. Of particular interest in such studies is that the TM doped In_2O_3 films have high carrier mobilities in spite of high carrier densities compared with those in tin-doped In_2O_3 (ITO). It will be desirable to achieve better conductivity due to the improvement in the mobility rather than in the electron density because of minimizing visible absorption and sharpening infrared reflectance [6].

Besides the excellent opto-electronic properties, doped In_2O_3 films can act as superconductors and thermoelectric materials. As to those examples, one of us (NM) reported detailed superconducting properties in ITO films [7], while it has also been reported that In_2O_3-ZnO composite films can show rather high thermoelectricity [8, 9] as well as superconductivity [10]. Since transparent-conductive materials and thermoelectric ones have common fundamental features in the sense that both materials show not only metallic but also semiconducting behaviors, it is of interest to study the relations between the two types of the materials.

We have recently studied opto-electronic properties in In_2O_3 films doped with cerium (ICO), obtaining a preliminary result that the ICO films could show relatively large thermoelectric power at room temperature [11]. It is shown that analyses of the thermoelectric power can provide important insights for characterizing thermoelectric materials [12, 13]. In this study, we report in detail experiments on the temperature dependence of the thermoelectric power $S(T)$ in ICO films. The results for $S(T)$ are discussed on the basis of a simple percolation model in which existing theories for $S(T)$ in both a simple metal and a semiconductor are combined.

II. EXPERIMENTAL

Films of ICO were prepared by dc magnetron sputtering with a ceramic target of In_2O_3-CeO_2 composite (99.99% in purity), the Ce doping level of which was ranged from 0 to 9 at.%. Sputtering deposition was carried out on Corning glass substrates kept at a temperature 473 K with a typical dc power of 10 W in Ar atmosphere of 10 Pa, resulting in film thickness of approximately 100 nm for one hour deposition time. X-ray diffraction measurements showed that all the films were in polycrystalline states. The lattice parameter of the cubic structure was increased upon Ce doping, due perhaps to larger ion radius of Ce^{4+} (0.092 nm) compared to that of In^{3+} (0.081 nm).

In order to characterize the ICO films, the following measurements were carried out. Electrical properties including the resistivity ρ, carrier density n and Hall mobility μ were measured at room temperature by the van der Pauw method with electric current 5 μA and magnetic field 0.6 T. The optical transmittance was measured with a spectrophotometer in the wavelength range of 240-2600 nm. Measurements on $S(T)$ were carried out using a liq-N_2 cryostat in the range of 100 K $\leq T \leq$ 300 K, by means of a differential method in a similar manner as in our previous reports [14, 15]. The temperature difference

*This paper was presented at the 6th International Symposium on Surface Science –Towards Nano, Bio and Green Innovation–, Tower Hall Funabori, Tokyo, Japan, December 11-15, 2011.
†Corresponding author: mori@oyama-ct.ac.jp
‡Present address: National Institute for Materials Science (NIMS), 1-1 Namiki, Tsukuba, Ibaraki 305-0044, Japan

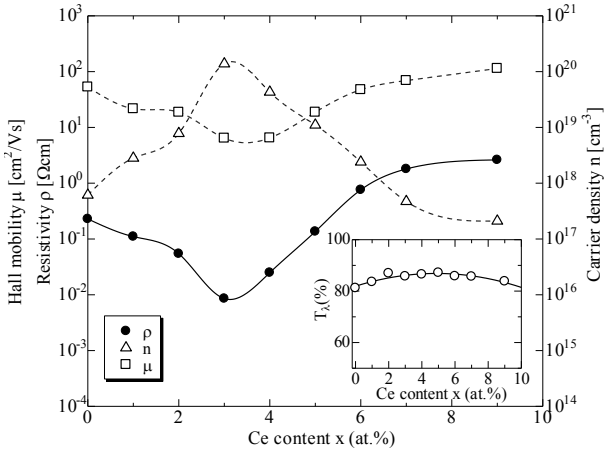

FIG. 1: The main panel displays the resistivity ρ, carrier density n and Hall mobility μ in ICO films as a function of the Ce content x. The inset displays the doping dependence of the optical transmittance T_λ averaged over the visible light region.

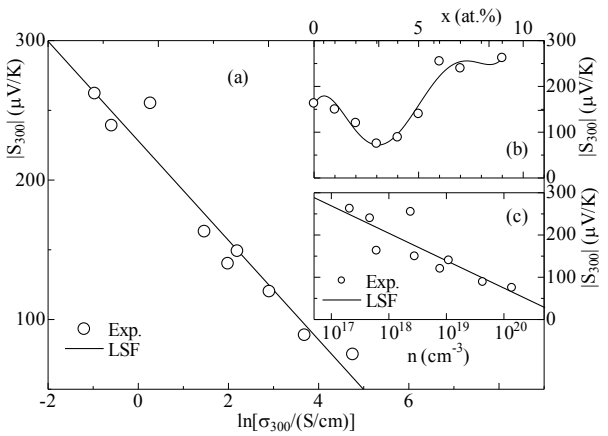

FIG. 2: Summaries of the thermoelectric power at room temperature in ICO films. The main panel (a) displays Jonker plots of S_{300} (absolute values) against the conductivity σ_{300} (in the logarithmic scale). The inset (b) displays the doping dependence of S_{300} while (c) displays S_{300} as a function of the carrier density n. The solid lines in the figures (a) and (c) represent the least squared fits to the data, while the line in (b) is drawn only for a guide to the eye.

across the film was kept to be a few K during the $S(T)$ measurements with copper-constantan thermocouples as sensors.

III. RESULTS AND DISCUSSION

A. Opto-electronic properties

Electrical and optical properties of the films under study are summarized in Fig. 1, where the main panel shows ρ, n and μ as a function of the Ce doping level x whereas the inset shows the doping dependence of the optical transmittance T_λ averaged over λ = 400-780 nm. All the films exhibit T_λ values between 80-90%, thus being rather transparent. As can be seen from Fig. 1, the variation in ρ is primary attributed to that in n rather than in μ. This result is at variance with the case of In_2O_3 films with TM-dopants, in which the enhancement in the mobility is observed even at the optimum doping level [3–5]. The lowest value in ρ upon Ce doping is attained at smaller impurity content in comparison to the case of Sn doping (i.e. ITO), as has been observable in the TM doping. The origin of such a feature may be traced back to the reason that the dopants of transition-metal and rare-earth metal elements can provides carriers only at lower doping levels up to a few percents, beyond which the strong interaction among dopants prevents from producing carriers [1].

B. Thermoelectric properties

In an ideal n-type semiconductor, the thermoelectric power S can be expressed as [8]

$$S = -a\left[\ln\left(N_{\rm c}/n\right) + L\right], \qquad (1)$$

where $a = k_{\rm B}/e \approx 86.2$ μV/K with the Boltzmann constant $k_{\rm B}$ and electronic charge $-e$, $N_{\rm C}$ is the effective density of states in the conduction band and L is a positive constant number. Combining Eq. (1) and the relation $\sigma = en\mu$ (with the conductivity σ), we obtain the formula

$$S = -a\ln(\sigma) + b, \quad b \equiv a\left[\ln\left(e\mu N_{\rm C}\right) + L\right], \qquad (2)$$

indicating that the plots of S against $\ln(\sigma)$ give a linear relation provided that values of μ in the system remain almost unchanged. This representation is known as the Jonker plots, and is often adopted as a useful way of characterizing thermoelectric materials [16]. The present results for thermoelectric properties are displayed in Fig. 2 in three different manners of representations. In the main panel (a), room-temperature values of the thermoelectric power S_{300} and conductivity σ_{300} are plotted in the Jonker fashion. The upper inset (b) and lower one (c) display the x-dependence of S_{300} and n-dependence of S_{300} in ICO films, respectively. Although the sign of S_{300} was negative as expected for an n-type semiconductor in all the present measurements, we have shown the absolute values of S_{300} in Fig. 2. Comparing Fig. 2(b) with Fig. 1 (the main part), we notice a qualitative similarity between ρ and S_{300} upon Ce doping. This is a general feature observed in standard semiconductors, indicating that free carriers play dominant roles in the ρ and S_{300} properties. Furthermore, a correlation between S_{300} and n shown in Fig. 2(c) suggests that the thermally activated charge carriers are responsible for observed thermoelectric properties. The nearly linear dependences observed in Figs. 2(a) and (c) indicate that relations between electrical conduction and thermoelectricity can be recognized qualitatively in terms of Eqs. (1) and (2), though ICO films are not exactly non-degenerated semiconductors. We have already reported that similar results are observable in thermoelectric properties of percolative oxide systems [15]. From the least squared fits (LSF) to the data (the solid lines), we obtain experimental values a = 228 and 282 μV/K for Eqs. (1) and (2), respectively. These values are significantly dif-

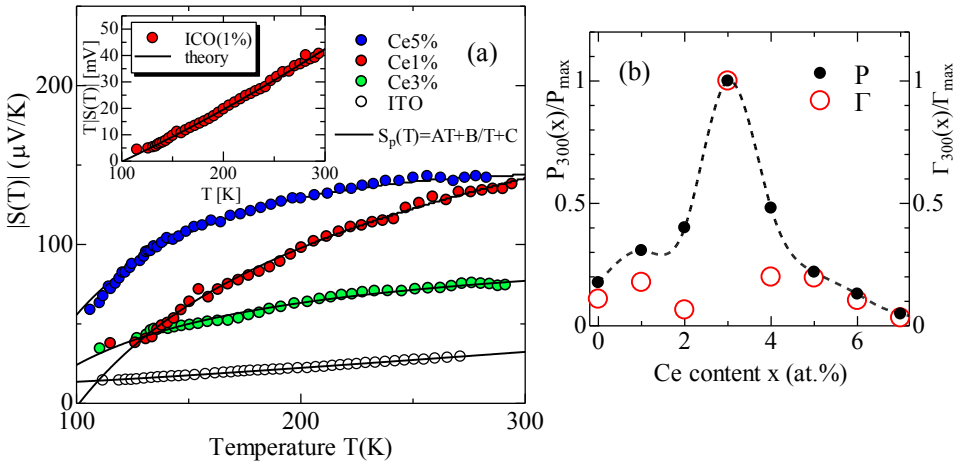

FIG. 3: (a) The main panel displays the temperature dependence of the thermoelectric power $S(T)$ (absolute values) in ICO films together with theoretical fits to Eq. (5). The inset displays an example for theoretical fits of $S(T)$ data in the ICO film with $x = 1$ at.%. (b) The Ce-doping dependence of the normalized percolation index Γ_{300} at room temperature. The corresponding results for the power factor P_{300} are also displayed.

ferent from the theoretical prediction $a = 86.2$ μV/K, indicating that the ICO films act as "effectively-ideal" semiconductors with renormalized factor a.

Next, let us present and discuss results for $S(T)$ measurements in the ICO films, which are displayed in Fig. 3(a). The T-linear dependence of the data for an ITO film also shown in the same figure for comparison is in agreement with the results reported by others [17]. It can be seen that for the ICO films with higher σ_{300} values $S(T)$ obeys the nearly T-linear dependence while $S(T)$ shows a downward curvature in the less conductive films. Overall features shown in Fig. 3(a) will remind us of the behaviors of $S(T)$ observed in metal-semiconductor percolation systems [15, 18, 19], for which cases a narrow conduction-band model [20] or a Boson-Fermion model [21] have been employed to explain the experimental data. In an attempt to interpret the present results, we propose a simple but useful tool for characterizing thermoelectric properties in systems covering metallic and semiconducting natures.

On the basis of a standard theory for non-generated semiconductors of the n-type, it is straightforward to obtain, from Eq. (1), the formula for $S_S(T)$ as

$$S_S(T) = -\frac{k_B}{e}\left(\frac{E_C - E_F}{k_B T} + L\right), \qquad (3)$$

where E_C is the energy level corresponding to the bottom of the conduction band and E_F is the Fermi level. On the other hand, $S(T)$ for a simple metal (or more generally speaking, "a Fermi liquid") is given by [22]

$$S_M(T) = -\frac{\pi^2 k_B}{3e} \cdot \frac{k_B T}{E_F}. \qquad (4)$$

Assuming that both $S_S(T)$ and $S_{M(T)}$ type contributions exist in a percolative system composed of metal and semiconductor materials, we express a total thermoelectric power as

$$S_P(T) = AT + (B/T) + C, \qquad (5)$$

TABLE I: Values of the fitting parameters in the $S(T)$ analyses for ICO films shown in Fig. 3(a).

ICO films x (%)	A 10^{-8} [V/K^2]	B 10^{-3} [V]	C 10^{-5} [V/K]
0	−20.8	13.5	−15.5
1	−15.9	16.8	−15.0
2	−8.51	3.29	−7.42
3	−1.27	7.56	−9.85
4	5.85	6.93	−12.7
5	15.3	17.8	−24.9
6	−8.55	5.28	−12.4
7	−30.8	−5.99	−3.39

where A, B and C are to be treated as fitting parameters. A similar expression has been obtained in a theoretical calculation for $S(T)$ based on the pseudo-gap model [23]. In order to determine values of these parameters, it is convenient to express the experimental data in the $T \cdot |S(T)|$ vs. T relation as shown in the inset of Fig. 3(a), where the solid line represents the least squared fit (LSF) to a quadratic equation $T \cdot |S_P| = |AT^2 + CT + B|$. The solid lines displayed in the main panel of Fig. 3(a) are obtained by the above-mentioned method, and can provide good descriptions of the experimental data.

Values of the fitting parameters A, B and C obtained from the theoretical fittings shown in Fig. 3(a) are displayed in Table I. It is important to make a discussion on these parameters to assure the validity of our analyses. Concerning the signs of these parameters, B is positive (except at $x = 7$ at.%) while C is negative upon Ce doping, resulting in negative values of the semiconducting contribution $(B/T) + C$ over the whole doping levels. These results are in agreement with the case of n type semiconductors with the degenerated nature where the condition $E_F > E_C$ is fulfilled. The highly resistive film with $x = 7$ at.% may be non-degenerated. It is therefore anticipated that Eq. (3) holds true also to degener-

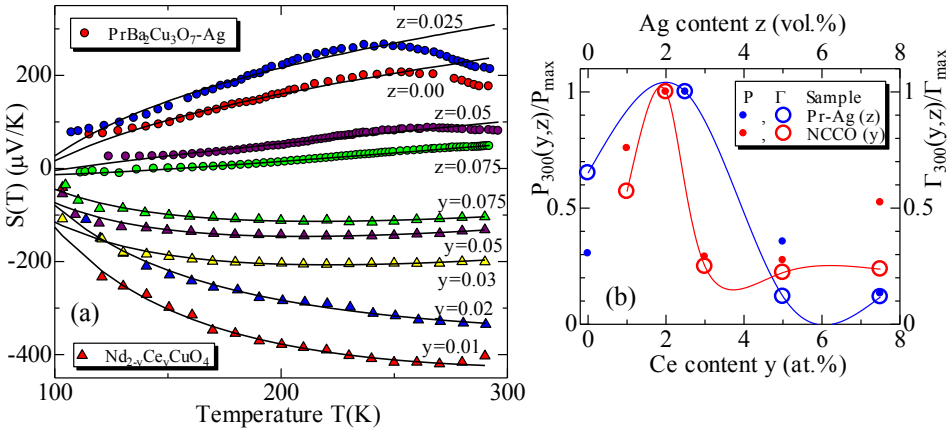

FIG. 4: (a) Results for $S(T)$ analyses in $Nd_{2-y}Ce_yO_4$ system (NCCO, triangles) with Ce atomic ratio $0 \leq y \leq 7.5\%$ and Ag-doped $PrBa_2Cu_3O_7$ system (Pr-Ag, circles) with Ag volume ratio $0 \leq z \leq 7.5\%$. The solid lines represent fits to Eq. (5). (b) The doping dependences of the normalized percolation index Γ_{300} and the power factor P_{300} at room temperature in NCCO and Pr-Ag systems.

ated semiconductors. On the other hand, A is negative at the lower and higher doping levels while positive at intermediated doping levels. Although the positive sign of A is inconsistent with Eq. (4) obtained from the free electron model, the metallic contribution AT in Eq. (5) can be regarded as something like a compensation term for a non-ideal character deviated from Eq. (3) since the contribution from the metallic term is rather smaller than that from the semiconducting term.

In a system where $S(T)$ properties are in the regimes of Eqs. (2) and (5), it is expected that the performance as thermoelectric materials becomes higher for a smaller metallic contribution (reduced A values) and a larger semiconducting contribution (enhanced B values). Therefore, we define the following parameter for charactering percolative thermoelectric materials:

$$\Gamma = |B/(AT^2)|, \tag{6}$$

for which we name "a percolation index". For the sake of Γ being dimensionless, we have included T^2 in Eq. (6). As a measure for estimating the performance of thermoelectric materials, one may evaluate, in general, a power factor defined as $P = S^2 \cdot \sigma$. Values of Γ and P at room temperature (denoted by Γ_{300} and P_{300}, respectively) are displayed as a function of the Ce content x in Fig. 3(b), where each parameter value is normalized by its maximum value ($\Gamma_{\max}$ or $P_{\max}$). It is to be noted that relations of Γ_{300} and P_{300} upon doping show a similar tendency, especially, both showing maximum at $x = 3\%$. Therefore, it is anticipated that the percolation index may play a role of a measure for characterizing thermoelectric materials in ceramic system. A percolation nature can be expected in physical properties of any ceramic films, and in fact percolation approaches have been reported successfully in the studies of electronic properties in ITO films [24, 25]. Finally, it is worth noting that we have obtained the maximum power factor $P_{\max} \approx 0.7$ (μW/cmK^2) in the ICO film with $x = 3$ at.%, which is comparable to values reported for In_2O_3-ZnO films possibly regarded as high-performance thermoelectric materials of the n-type [8, 9].

C. Related results for $S(T)$ in bulk ceramics

In order to confirm the role of the index Γ defined by Eq. (6), here we reanalyze, on the basis of Eq. (5), our previous experimental data on $S(T)$ in bulk ceramic systems related to copper-oxide superconductors. Results for the analyses of $S(T)$ data are displayed in Fig. 4(a) for the cases of $Nd_{2-y}Ce_yO_4$ (NCCO) [14] and Ag-doped $PrBa_2Cu_3O_7$ (Pr-Ag) [15] which are known as electron-doped (n-type) and hole-doped (p-type) materials, respectively. In the former system, Ce was substituted for Nd in the atomic ratio y (at.%) while Ag was added in the volume fraction z (vol.%) in the latter one. The solid lines along with the data (plots) represent fits to Eq. (5), showing satisfactory agreement between theory and experiment in much the same ways as for other theoretical models. The signs of B, C and $(B/T) + C$ in the NCCO system are in accordance with those in the ICO films, whereas the opposite signs in those parameter values are obtained for the p-type Pr-Ag system. As regards values of A, the positive sign is always obtained in both of the systems, thus being inconsistent with the known result in the standard theory as far as n-type materials are concerned. Although there are some contradictions in the signs of the parameters, we believe that our simple model based on Eq. (5) is essentially valid for the $S(T)$ analyses in the systems under study. In Fig. 4(b), we compare the relations between Γ_{300} and P_{300} upon impurity doping in both NCCO and Pr-Ag systems. Looking at the behavior shown in this figure together with that in Fig. 3(b), we are of the opinion that the behaviors in Γ_{300} and P_{300} upon doping resemble each other, and that Γ_{300} could be a useful factor to characterize thermoelectric materials of ceramic systems.

IV. CONCLUSIONS

We have investigated thermoelectric properties in ICO films with Ce content x up to 9 at.% prepared by dc magnetron sputtering. The ICO films under study have visi-

ble light transmittance more than 80%, while showing the lowest resistivity 8.3 mΩcm at $x = 3$ at.% but otherwise having higher resistivity values. The variation in the resistivity upon doping is mainly attributed to the increase in the carrier density rather than that in the Hall mobility, in contrast to the cases of the TM dopants. The thermoelectric power at room temperature upon Ce doping exhibits a tendency similar to that of the carrier density, the feature of which can be reconciled with a standard theory of a semiconductor, and therefore following the linear dependence in the Jonker representation.

The measurements on $S(T)$ have been carried out in the temperature range of 100 K $\leq T \leq$ 300 K. In order to interpret the results for $S(T)$, we have adopted a simple percolation model in which $S(T)$ is composed of both metallic and semiconducting contributions, showing good agreement between theory and experiment. With the aid of values for fitting parameters in the above-mentioned model, we could define an index, characteristic of percolation systems, the doping dependence of which may mutually compromise with the power factor. Similar results have also been obtained in the analyses of $S(T)$ for bulk composites of n-type $Nd_{2-y}Ce_yO_4$ and p-type Ag-doped $PrBa_2Cu_3O_7$ known as typical percolation systems. Summarizing very briefly, the ICO films can be regarded as a candidate of transparent-conductive thermoelectric materials.

[1] T. Minami, *Developments of Transparent Conductive Films III* (CMC Publishing Co. Ltd., Tokyo, 2008).
[2] T. Maruyama and T. Tago, Appl. Phys. Lett. **64**, 1395 (1994).
[3] C. Warmsingh, Y. Yoshida, D. W. Readey, C. W. Teplin, J. D. Perkins, P. A. Parilla, L. M. Gedvilas, B. M. Keyes, and D. S. Ginley, J. Appl. Phys. **95**, 3831 (2004).
[4] M. F. A. M. van Hest, M. S. Dabney, J. D. Perkins, D. S. Ginley, and M. P. Taylor, Appl. Phys. Lett. **87**, 032111 (2005).
[5] T. Koida and M. Kondo, Appl. Phys. Lett. **89**, 082104 (2006).
[6] T. J. Coutts, D. L. Young, and X. Li, MRS Bull. **25**, 58 (2000).
[7] N. Mori, J. Appl. Phys. **73**, 1327 (1993).
[8] S. Hirano, S. Isobe, T. Tani, N. Kitamura, I. Matsubara, and K. Koumoto, Jpn. J. Appl. Phys. **41**, 6430 (2002).
[9] Y. Orikasa, N. Hayashi, and S. Muranaka, J. Appl. Phys. **103**, 113703 (2008).
[10] B. Shinozaki, N. Kokubo, S. Takada, T. Yamaguti, K. Yamada, K. Makise, K. Yano, K. Inoue, and H. Nakamura, J. Phys.: Conf. Series **150**, 052237 (2009).
[11] D. Tsukada, I. Maezawa, K. Idebuchi, F. Kano, and N. Mori, Proceedings of the 6th International Symposium on Transparent Oxide Thin Films for Electronics and Optics (TOEO-6), p. 300 (2009).
[12] A. Ishida, D. Cao1, S. Morioka, M. Veis, Y. Inoue, and T. Kita, Appl. Phys. Lett. **92**, 182105 (2008).
[13] P. Sun, N. Oeschler, S. Johnsen, B. B. Iversen, and F. Steglich, Appl. Phys Express **2**, 091102 (2009).
[14] N. Mori, T. Kameyama, H. Enomoto, H. Ozaki, Y. Takano, and K. Sekizawa, J. Alloys Compd. **408-412**, 1222 (2006).
[15] N. Mori, H. Okano, and A. Furuya, Phys. Status Solidi A **203**, 2828 (2006).
[16] M.-Y. Su, C. E. Elsbernd, and T. O. Mason, Physica C **160**, 114 (1989).
[17] Z Q. Li and J. J. Lin, J. Appl. Phys. **96**, 5918 (2004).
[18] X. H. Chen, T. F. Li, M. Yu, K. Q. Ruan, C. Y. Wang, and L. Z. Cao, Physica C **290**, 317 (1997).
[19] D. R. Sita and R. Singh, Physica C **296**, 21 (1998).
[20] V. E. Gasumyants, E. V. Vladimirskaya, and I. B. Patrina, Phys. Solid State **39**, 1352 (1997).
[21] S. Ikegawa, T. Wada, T. Yamashita, A. Ichinose, K. Matsuura, K. Kubo, H. Yamauchi, and S. Tanaka, Phys. Rev. B **43**, 11508 (1991).
[22] A. A. Abrikosov, *Fundamentals of the Theory of Metals* (North-Holland, Amsterdam, 1988).
[23] Q. M. Zhang, X. S. Xu, X. N. Ying, A. Li, Q. Qiu, Y. N. Wang, G. J.Xu, and Y. H. Zhang, Physica C **337**, 277 (2000).
[24] K. Shida, R. Sahara, H. Mizuseki, and Y. Kawazoe, J. Japan Inst. Metals **73**, 171 (2009).
[25] J. Ueno, R. Itagaki, K. Idebuchi, and N. Mori, Abstract in Thin Film Material & Device Meeting (TFMD-6) Nara, p. 198 (2009).